

A CFD approach to study the local importance of aggregation in precipitation

*Original*

A CFD approach to study the local importance of aggregation in precipitation / Marchisio, Daniele; Fox, R.; Barresi, Antonello; Baldi, Giancarlo. - STAMPA. - (2000), pp. 363-373. ( 7th International Conference on Multiphase Flow in Industrial Plants Bologna (Italy) 13-15 September 2000).

*Availability:*

This version is available at: 11583/1407617 since: 2016-09-15T23:42:13Z

*Publisher:*

AIDIC & ANIMP

*Published*

DOI:

*Terms of use:*

This article is made available under terms and conditions as specified in the corresponding bibliographic description in the repository

*Publisher copyright*

(Article begins on next page)

**A CFD APPROACH TO STUDY THE LOCAL IMPORTANCE  
OF AGGREGATION IN PRECIPITATION**

**D.L. Marchisio, R.O. Fox, A.A. Barresi and G. Baldi**

363-373

**ANIMP**

Multiphase Flow  
Engineering Section

**UNIVERSITY OF BOLOGNA**

**DIEM**

Department  
of Mechanical  
Engineering

**AIDIC**

Italian Association  
of Chemical Engineering

**Faculty of Engineering  
Bologna, Italy  
September 13-15, 2000**

**Seventh International Conference**

**MULTIPHASE FLOW IN INDUSTRIAL PLANTS**

## SCIENTIFIC COMMITTEE

**Giancarlo Baldi**

*Politecnico di Torino*

**Ugo Biliardo**

*Università di Roma*

**Gian Piero Celata**

*Enea Casaccia, Roma*

**Giorgio Donsì**

*Università di Salerno*

**Dario Ercolani**

*Snamprogetti S.p.A., Centro di Fano*

**Sergio Fabbri**

*Università di Bologna*

**Giovanna Ferrari**

*Università di Salerno*

**Brunello Formisani**

*Università della Calabria*

**Francesco Ferrini**

*Techfem S.r.l., Fano*

**Giancarlo Giacchetta**

*Università di Ancona*

**Giovanni Guglielmini**

*Università di Genova*

**Carlo Lombardi**

*Politecnico di Milano*

**Barbara Mazzarotta**

*Università di Roma*

**Agostino Mazzoni**

*ENI S.p.A. - Div. Agip, Milano*

**Arrigo Pareschi**

*Università di Bologna*

**Cesare Saccani**

*Università di Bologna*

**Alessandro Terenzi**

*Snamprogetti S.p.A., Centro di Fano*

## ORGANIZING COMMITTEE

**Cesare Saccani**, *Università di Bologna*

**Claudio Alimonti**, *Università La Sapienza, Roma*

**Simone Spadolini**, *Techfem S.r.l., Fano*

**Francesco Visco**, *ANIMP, Milano*

**Anna Valenti**, *ANIMP, Milano*

## A CFD approach to study the local importance of aggregation in precipitation

D.L. Marchisio<sup>† 1</sup>, R.O. Fox<sup>‡</sup>, A.A. Barresi<sup>†</sup> and G. Baldi<sup>†</sup>

<sup>†</sup>Dip. Scienza dei Materiali ed Ingegneria Chimica  
Politecnico di Torino

C.so Duca degli Abruzzi 24, 10129, Torino, Italy

<sup>‡</sup>Dept. of Chemical Engineering

Iowa State University

2114 Sweeney Hall, Ames, IA 50011, USA

### Abstract

Precipitation of sparingly soluble salts is a mixing sensitive process that involves nucleation of the solid phase and various growth mechanisms. Two different growth mechanisms can be considered. The first one is the growth of the crystals from solution while the second one is growth from aggregation of smaller particles. Depending on the operating conditions different mechanisms control the crystal growth and thus morphology and size of the crystal. Experimental evidence shows that under certain conditions also in dilute systems aggregation takes place, forming smaller aggregates with various shapes. In this work a finite mode probability density function (pdf) coupled with a CFD code (FLUENT) has been used to model precipitation and the population balance has been solved in term of the moments of the crystal size. The results show that under these operating conditions the mean crystal size and the total number of particles are slightly affected by aggregation, but locally the crystal concentration is high enough to give an appreciable aggregation rate.

### 1 Introduction

During precipitation from solution several phenomena may occur, namely: nucleation, growth, aggregation and breakage. The first step is responsible for the formation of crystal nuclei. The new particles so formed can grow following different mechanisms, such as growth from solution or aggregation of smaller particles, whereas collision between particles and reactor walls or impeller may cause breakage, resulting in a reduction of particle size. Most of the time, the final product has to fulfil specific requirements on crystal size distribution (CSD) and crystal morphology.

Since the mixing time scale is comparable with the reaction time scale, the process is controlled both by precipitation kinetics and mixing. Several authors have studied the influence of mixing on the final CSD and crystal morphology and several modelling approaches have been adopted. Baldyga and Orciuch (1999) studied the turbulent precipitation of barium sulphate in a tubular reactor and compared the experimental data with the model predictions. In this work they used Computational Fluid Dynamic (CFD) coupled with different micromixing models, such as the presumed probability density function ( $\beta$ -pdf) and multi-environment model. Piton *et al.* (2000) studied the turbulent precipitation in the same reactor using CFD coupled with a multi-environment

<sup>1</sup>Corresponding author: e-mail: marchis@athena.polito.it; fax: +390115644699

micromixing model, and compared model predictions with results from other authors (Baldyga and Orciuch, 1997). Almost all modelling works appearing in the literature completely neglect the role of aggregation and breakage in precipitation. Whereas for breakage this assumption might be reasonable, numerous experimental studies have shown the important role of aggregation. Philips *et al.* (1999), working in a single-feed semi-batch precipitator, from observation of crystals with SEM found that under certain conditions particles form aggregates. Pagliolico *et al.* (1999), working with a continuous Couette type precipitator, found complex aggregates, named roses, probably formed by high local values of reactant concentration. The aim of this work is to study the effect of aggregation on turbulent precipitation in a tubular reactor. The reactor is modeled using a commercial CFD code (FLUENT) and the sub-grid scale is modeled using the multi environment approach. Perikinetik aggregation has been included in the model using the transformed population balance, under some simplifications.

## 2 Micromixing model

The multi-environment micromixing model divides each grid of the computational domain in  $N$  environments. This approach is equivalent to a discretization of the composition pdf in a finite set of delta functions (Fox, 1998):

$$f_{\phi}(\psi; \mathbf{x}, t) \equiv \sum_{n=1}^N p_n(\mathbf{x}, t) \prod_{\alpha=1}^m \delta(\psi_{\alpha} - \phi_{\alpha}^{(n)}(\mathbf{x}, t)) \quad (1)$$

where  $f_{\phi}(\psi; \mathbf{x}, t)$  is the joint PDF of all scalars (e.g., concentrations, moments, etc.) appearing in the precipitation model,  $p_n(\mathbf{x}, t)$  is the probability of mode  $n$  (i.e., the volume fraction of Environment  $n$ ),  $\phi_{\alpha}^{(n)}(\mathbf{x}, t)$  is the value of scalar  $\alpha$  corresponding to mode  $n$ ,  $N$  is the total number of modes, and  $m$  is the total number of scalars. Piton *et al.* (2000) showed that three environments are sufficient to work with good accuracy. Using three environments with the unpremixed chemical reaction  $A + B \rightarrow C$ , Environment 1 contains pure A, Environment 2 contains pure B, and Environment 3 contains mixed reactants (reaction occurs in this Environment).

The Reynolds-averaged transport equations for the volume fractions of Environments 1 and 2 are given by (repeated indices imply summation):

$$\frac{\partial p_1}{\partial t} + \frac{\partial}{\partial x_i} (\langle u_i \rangle p_1) = \frac{\partial}{\partial x_i} \left( \Gamma_t \frac{\partial p_1}{\partial x_i} \right) + \gamma_t p_3 - \gamma_s p_1 (1 - p_1), \quad (2)$$

$$\frac{\partial p_2}{\partial t} + \frac{\partial}{\partial x_i} (\langle u_i \rangle p_2) = \frac{\partial}{\partial x_i} \left( \Gamma_t \frac{\partial p_2}{\partial x_i} \right) + \gamma_t p_3 - \gamma_s p_2 (1 - p_2), \quad (3)$$

where  $p_3 = 1 - p_1 - p_2$ ,  $\langle u_i \rangle$  is the mean velocity in the  $i^{th}$  direction,  $\Gamma_t$  is the turbulent diffusivity modeled as

$$\Gamma_t = \frac{C_{\mu}}{Sc_t} \frac{k^2}{\epsilon}, \quad (4)$$

where  $C_{\mu} = 0.09$  and  $Sc_t = 0.7$ , whereas  $\gamma_s$  and  $\gamma_t$  are respectively the micromixing rate and the spurious dissipation rate. The micromixing term  $\gamma_s$  can be expressed in terms of the turbulent frequency ( $\epsilon/k$ ) as follows

$$\gamma_s = C_{\phi} \epsilon / k, \quad (5)$$

where  $C_\phi$  for a fully developed scalar field is of order of unity. Generally for environment  $n$  it is possible to define a local concentration denoted by  $\phi_\alpha^{(n)}$ , whereas the weighted concentration  $s_\alpha^{(n)}$  is defined by

$$s_\alpha^{(n)} = \phi_\alpha^{(n)} p_n. \quad (6)$$

The transport equation for the weighted concentration of scalar  $\alpha$  in Environment 3 is

$$\frac{\partial s_\alpha^{(3)}}{\partial t} + \frac{\partial}{\partial x_i} (\langle u_i \rangle \phi_\alpha^{(3)}) = \frac{\partial}{\partial x_i} \left( \Gamma_t \frac{\partial s_\alpha^{(3)}}{\partial x_i} \right) - \gamma_i p_3 (\phi_\alpha^{(1)} + \phi_\alpha^{(2)}) + \quad (7)$$

$$\gamma_s p_1 (1 - p_1) \phi_\alpha^{(1)} + \gamma_s p_2 (1 - p_2) \phi_\alpha^{(2)} + p_3 S_\alpha(\phi^{(n)}),$$

where  $\phi_\alpha^{(1)}$  and  $\phi_\alpha^{(2)}$  are the local concentrations in Environments 1 and 2 (that do not need a transport equation, because no reaction occurs in these environments), and  $S_\alpha(\phi^{(n)})$  is the chemical source term. Note that  $\gamma_t$  is required to eliminate spurious scalar dissipation, resulting from the finite-mode representation, but because the relative importance of this term in a tubular reactor is small, in this work this term has been neglected.

### 3 Population balance

The population balance is a continuity statement based on the number density function  $n(L; \mathbf{x}, t)$ , and is given as (Randolph and Larson, 1988)

$$\frac{\partial n}{\partial t} + \frac{\partial}{\partial x_i} (\langle u_i \rangle n) + \frac{\partial}{\partial L} (Gn) = \frac{\partial}{\partial x_i} \left( \Gamma_t \frac{\partial n}{\partial x_i} \right) + B(n) - D(n) \quad (8)$$

where  $G$  is the growth rate,  $B$  and  $D$  are respectively the birth and the death rate due to aggregation and  $L$  is the crystal dimension. This equation has to be applied only in Environment 3 because in this environment reaction/particle formation occurs. Rivera and Randolph (1978) suggested to use the moment transformation to convert this intractable set of equations. The first four moments are of particular interest, since they are related to the total number particle density ( $N_t = m_0$ ), the total particle area ( $A_t = k_a m_2$ ) and the total solid volume ( $V_t = k_v m_3$ ) by shape factors ( $k_a, k_v$ ) that depend on particle morphology. Using this approach the mean crystal size can be written as follows:

$$d_{32} = \frac{m_3}{m_2}, \quad (9)$$

and the solid concentration is given by

$$c_c = \frac{\rho k_v m_3}{M}, \quad (10)$$

where  $\rho$  is the crystal density,  $k_v$  is the volume shape factor, and  $M$  is the molecular weight of the crystal. The chemical source term appearing in Eq. 7 can be expressed in terms of  $m_2$  and  $G$  as follows:

$$S(\phi^{(n)}) = \frac{\rho k_a m_2 G}{2M}. \quad (11)$$

The transport equation for the  $j^{th}$  moment is:

$$\frac{\partial s_j^{(3)}}{\partial t} + \frac{\partial}{\partial x_i} (\langle u_i \rangle s_j^{(3)}) = \frac{\partial}{\partial x_i} \left( \Gamma_t \frac{\partial s_j^{(3)}}{\partial x_i} \right) + p_3 J(\phi_\alpha^{(3)}) (0)^j + G(\phi_\alpha^{(3)}) s_{j-1}^{(3)} + \quad (12)$$

$$p_3 \left[ \bar{B}_j(m_j^{(3)}) - \bar{D}_j(m_j^{(3)}) \right]$$

where  $s_j^{(3)} = m_j^{(3)} p_3$  is the weighted  $j^{th}$  moment of the number density function and  $\bar{B}_j$  and  $\bar{D}_j$  are the moments of birth and death rate due to aggregation. The model equations are defined once expressions for nucleation, growth, birth and death rate are found, and then can be added to FLUENT as user-defined scalars. For every user-defined scalar a transport equation of the form

$$\rho \frac{\partial \phi_k}{\partial t} + \frac{\partial}{\partial x_i} \left( \rho \langle u_i \rangle \phi_k - \rho \Gamma_k \frac{\partial \phi_k}{\partial x_i} \right) = S_{\phi_k} \quad (13)$$

is solved, where  $\phi_k$  is the  $k^{th}$  scalars,  $\rho$  is the fluid density and  $\Gamma_k$ , and  $S_{\phi_k}$  are the diffusivity and the source term for the  $k^{th}$  scalar, respectively (for details see Fluent User's Guide, 1990). In this work the diffusivity  $\Gamma_k$  has been set equal to the turbulent diffusivity ( $\Gamma_t$ ) for all scalars.

### 3.1 Nucleation and growth

The problem of a particulate system governed by nucleation and growth is well known and for barium sulphate several kinetic expressions have appeared in literature. In this work the expressions proposed by Baldyga and co-workers (1995) have been used. For the nucleation rate the supplied expression is:

$$J(\phi_A, \phi_B) = \begin{cases} 2.83 \times 10^{10} \Delta c^{1.775} & (1/\text{m}^3\text{s}) \quad \text{for} \quad \Delta c < 10 \text{ mol}/\text{m}^3 \text{ (heterogeneous)} \\ 2.53 \times 10^{-3} \Delta c^{15} & (1/\text{m}^3\text{s}) \quad \text{for} \quad \Delta c > 10 \text{ mol}/\text{m}^3 \text{ (homogeneous)} \end{cases} \quad (14)$$

where  $\Delta c = \sqrt{\phi_A \phi_B} - \sqrt{k_s}$ , and  $k_s$  is the solubility product of barium sulphate (at room temperature  $k_s = 1.14 \times 10^{-4} \text{ mol}^2/\text{m}^6$ ).

For the growth rate a two-step diffusion-absorbition model (Nielsen, 1984) was used, and gives the following expression:

$$G(\phi_A, \phi_B) = 5.8 \times 10^{-8} \Delta c^2 = k_d (\phi_A - \phi_{As}) = k_d (\phi_B - \phi_{Bs}) \quad (\text{m/s}) \quad (15)$$

where  $k_d$  is the mass transfer coefficient that can be estimated from the theory of mass transfer to micro particles (Nagata and Nishikawa, 1972). Using this approach,  $k_d$  has been fixed to be equal to  $1.5 \times 10^{-8} \text{ (m/s)(m}^3/\text{mol)}$ . Baldyga and Orciuch (1997) reported the crystal morphology to be in the range  $8.17 < k_a < 348$ , where 8.17 is the factor for a well-formed rectangular crystal and 348 is the factor for a pyramidal crystal formed by surface nucleation. Because they found the best agreement with their experimental data by using a shape factor equal to 348, this value will also be used in this work.

### 3.2 Aggregation

The study of aggregation starts from the work of Smoluchowski (1917) that first defined the birth and the death rate for a discrete system made by interacting monomers. The equations can be rewritten for a continuous system in terms of the particle volume as follows:

$$B'(v) = \frac{1}{2} \int_0^v \beta'(v - \epsilon, \epsilon) n'(v - \epsilon) n'(\epsilon) d\epsilon, \quad (16)$$

$$D'(v) = n'(v) \int_0^\infty \beta'(v, \epsilon) n'(\epsilon) d\epsilon, \quad (17)$$

where  $n'(v)$  is the particle number density with particle volume as internal coordinate and  $\beta'(v, \epsilon)$  is the aggregation kernel, that is a measure of the frequency of collision of the particles of volume  $v$  and  $\epsilon$  that are successful in producing a particle of volume  $v + \epsilon$ . In order to be able to introduce these terms in the moment transport equations, a further passage is needed. It is easy to show that Eqs. 16 and 17 expressed in a length-based form are as follows:

$$B(L) = \frac{L^2}{2} \int_0^L \frac{\beta [(L^3 - \lambda^3)^{1/3}, \lambda] n [(L^3 - \lambda^3)^{1/3}, \lambda] n(\lambda) d\lambda}{(L^3 - \lambda^3)^{2/3}}, \quad (18)$$

$$D(L) = n(L) \int_0^\infty \beta(L, \lambda) n(\lambda) d\lambda. \quad (19)$$

Application of the moment transforms to Eqs. 18 and 19 yields

$$\bar{B}_j = \int_0^\infty \frac{L^{2+j}}{2} \int_0^L \frac{\beta [(L^3 - \lambda^3)^{1/3}, \lambda] n [(L^3 - \lambda^3)^{1/3}, \lambda] n(\lambda) d\lambda dL}{(L^3 - \lambda^3)^{2/3}}, \quad (20)$$

$$\bar{D}_j = \int_0^\infty L^j n(L) \int_0^\infty \beta(L, \lambda) n(\lambda) d\lambda dL. \quad (21)$$

The problem is closed if  $\bar{B}_j$  and  $\bar{D}_j$  are expressed in terms of the moments of the CSD. In order to supply this relationship some knowledge of the aggregation kernel is needed. The form of the aggregation kernel generally depends on the type of aggregation involved. Since the particle dimension in this case is lower than  $1 \mu m$  only perikinetic aggregation is considered. Under this assumption the aggregation kernel is a function of the fluid properties and the size of the colliding particles. In this work only interaction between particles of about the same size is considered. In this case we will make use of the assumption of a constant aggregation kernel. Thus in all equations  $\beta(L, \lambda)$  will be replaced by  $\beta_0$ . Putting  $u^3 = L^3 - \lambda^3$  and reversing the order of integration, Eq. 20 becomes (Hounslow *et al.*, 1988)

$$\bar{B}_j = \frac{\beta_0}{2} \int_0^\infty n(\lambda) \int_0^\infty (u^3 + \lambda^3)^{j/3} du d\lambda. \quad (22)$$

This double integral may be expanded in terms of the moments of the CSD only if  $j/3$  is an integer (i.e.,  $j=0,3$ ). In these two cases the resulting expressions are:

$$\bar{B}_0 = 1/2 \beta_0 m_0^2, \quad (23)$$

Table 1: Geometric parameter for the tubular reactor

Main tube inner diameter, mm	32
Injection tube outer diameter, mm	2.5
Injection tube inner diameter, mm	1.8
Main tube length, mm	1240
Injection tube length, mm	240

$$\bar{B}_3 = \beta_0 m_0 m_3. \quad (24)$$

For  $j = 1, 2$  the integral can be solved if  $(u^3 + \lambda^3)^{j/3}$  is replaced by its Taylor series

$$(u^3 + \lambda^3)^{j/3} = u^j (1 + x^3)^{j/3} = u^j [a_1 + a_2(x-1) + a_3(x-1)^2 + \dots + a_n(x-1)^n], \quad (25)$$

where  $a_n$  may be written in terms of the  $n^{\text{th}}$  derivative of the function  $(1+x^3)^{j/3}$ . This assumption is valid if  $x$  is very close to one, this implies that the particle sizes  $L$  and  $\lambda$  appearing in Eqs. 20 and 21 are almost the same. Using this approach the following equation is obtained

$$\bar{B}_j = \beta_0 b_j m_0 m_j, \quad (26)$$

$b_1$  and  $b_2$  might be calculated analytically, but in this work their value has been chosen in such a way to force the simplified model to follow the analytical solution, found by Gelbard and Seinfeld (1978), for an exponential CSD and constant aggregation kernel. Using this approach  $b_1 = 2/3$  and  $b_2 = 5/6$ . For the death rate, under the assumption of constant aggregation kernel, Eq. 21 is transformed as follows

$$\bar{D}_j = \beta_0 m_0 m_j. \quad (27)$$

We have to highlight that for  $j = 3$  the sum of birth and death rate due to aggregation is null, because aggregation does not change the total solid volume.

### 3.3 Results and discussion

Barium sulphate precipitation was studied in a tubular reactor (Baldyga and Orciuch, 1997, 1999). In Table 1 the reactor geometric parameters are reported. The CFD simulations were carried out in an axisymmetric geometry using a grid with a finer resolution near the reactor inlet. The velocity of the two feed-streams is the same and is equal to 2 m/s. This flow rate gives  $Re=64000$ . The feed-stream concentrations were  $\phi_A^{(1)} = 500 \text{ mol/m}^3$  (barium chloride) and  $\phi_B^{(2)} = 7.5 \text{ mol/m}^3$  (sodium sulphate). The steady-state simulations were carried out solving the flow field using the standard  $k - \epsilon$  model first, and then the volume fractions of Environments 1 and 2. The last step was the solution of the transport equations for the reacting scalars in Environment 3.

The volume fraction of Environment 1 is non-zero only in a small region near the injection zone, whereas the volume fraction of Environment 2 is non-zero in the annular region. The interaction between Environments 1 and 2 creates Environment 3, in which reaction occurs. As soon as the two streams mix together, nucleation takes place. The high local value of supersaturation gives a high peak of nucleation rate. The maximum is located very close to the small tube inlet, and a high number of particles is created in this region. Due to turbulent mixing the local reactant concentrations decrease very rapidly and because of its non-linear nature, the nucleation rate decreases faster.

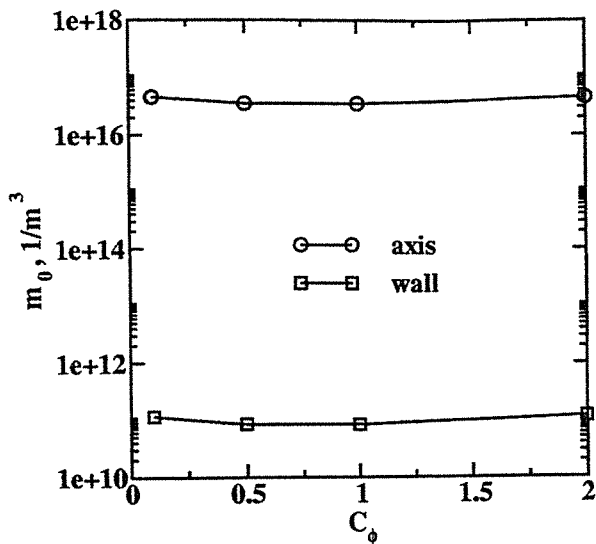


Figure 1: Effect of  $C_\phi$  on total number particle density at the reactor outlet.

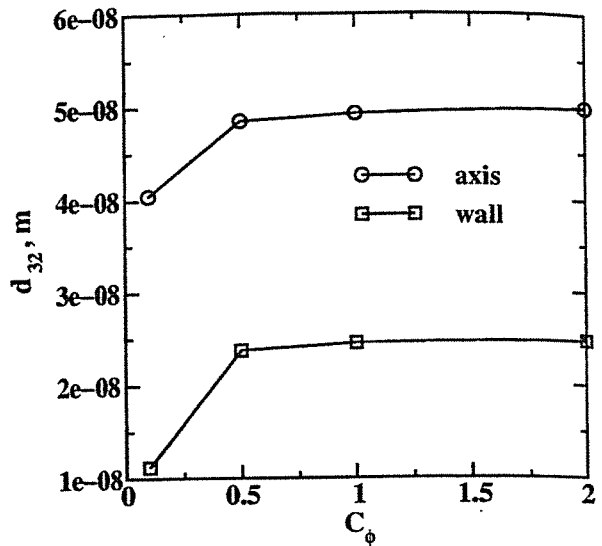


Figure 2: Effect of  $C_\phi$  on mean crystal size at the reactor outlet.

The influence on the final solution of the model parameters  $C_\phi$  and  $\beta_0$  was considered. Reactant A is in Environment 1 and is injected through the small tube, while reactant B is in Environment 2 and is led by the main tube.

In Fig. 1 the total particle number density at the reactor outlet for several values of  $C_\phi$  is reported. A shallow minimum located at  $C_\phi = 0.5$  was found; in fact, a decrease in  $C_\phi$  slows down mixing, and is responsible for shifting the maximum of the profile along the axial direction, and reducing the mixing between the two reactants (i.e., reducing the overall nucleation rate). After the injection zone the nucleation rate is very low, whereas the growth rate is high enough to make crystals grow. Also the mean crystal size is affected by the choice of  $C_\phi$  (see Fig. 2). Decreasing  $C_\phi$  the mean crystal size decreases due to the poor mixing that reduces the growth rate. These results show that, in this range, the effect of the micromixing constant on the overall process is small. As done in a previous work (Marchisio *et al.*, 2000), in order to take into account the fact that the scalar field near the injection point is not fully-developed  $C_\phi$  has been fixed lower than unity ( $C_\phi = 0.5$ ).

In Fig. 3 the axial profiles of total number density are reported for several value of  $\beta_0$ . As it is possible to see for all the values the profiles show a maximum due to the high local nucleation rate. Increasing  $\beta_0$  a lower peak of total number density is found, due to enhanced aggregation that reduces the number of particles. This effect is localized in the small region near the inlet of the small tube, but is also appreciable far from this point. Plotting the radial profiles of total number density at the reactor outlet (Fig. 4), it is possible to see that an increase in  $\beta_0$  results in a lower number of particles. For all the aggregation kernel values the radial profile has a maximum on the reactor axis, due to the fact that the highest value of nucleation rate is localized in this zone of the reactor. The aggregation rate has also an effect on the mean crystal size; in fact, plotting the radial profiles of the mean crystal size for several  $\beta_0$  (Fig. 5), it is clear that an increase in  $\beta_0$  results in particles with bigger dimension. Bigger particles are located near the reactor axis because also the growth rate has the highest value in this zone of the reactor.

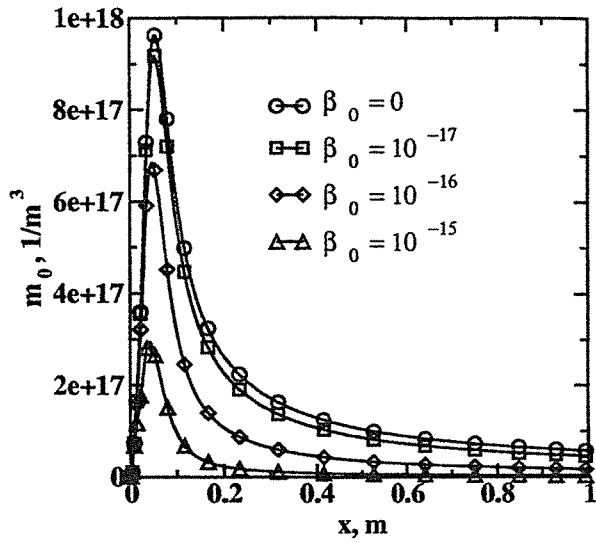


Figure 3: Axial profile of total number density for several values of aggregation kernel  $\beta_0$ .

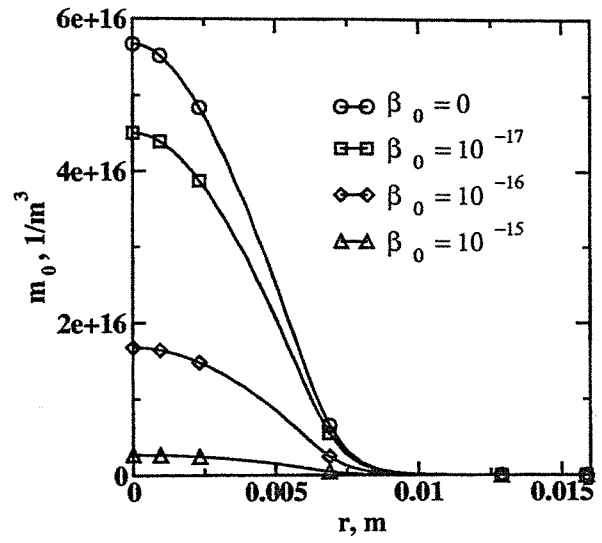


Figure 4: Radial profile of total number density at reactor outlet for several values of aggregation kernel  $\beta_0$ .

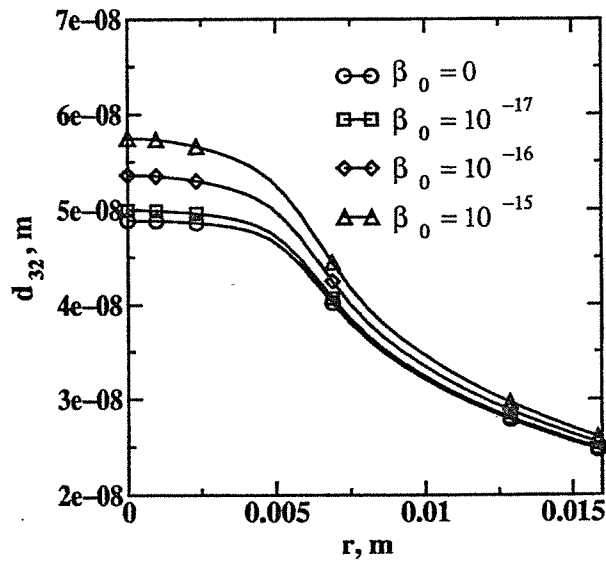


Figure 5: Radial profile of mean crystal size at reactor outlet for several values of aggregation kernel  $\beta_0$ .

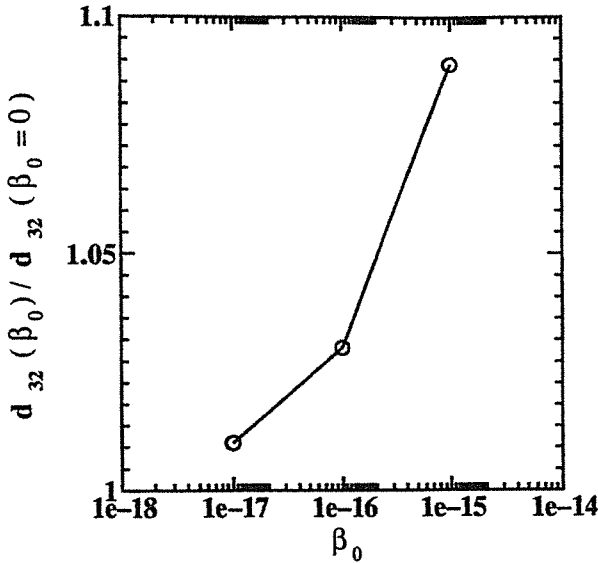


Figure 6: Relative variation of the radial-averaged mean crystal size against  $\beta_0$ .

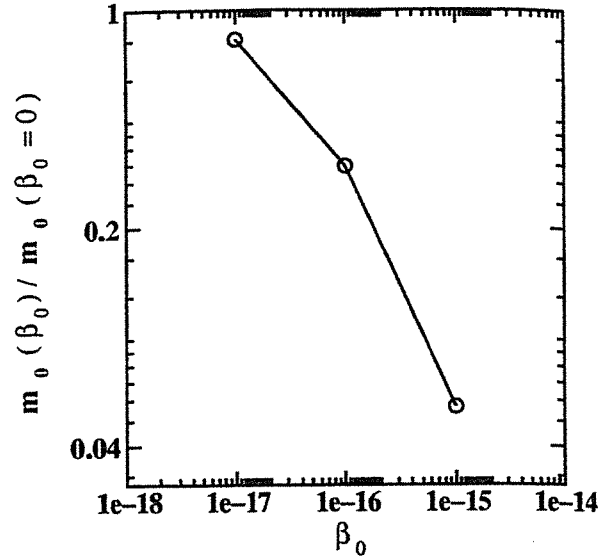


Figure 7: Relative variation of the radial-averaged total number density against  $\beta_0$ .

In perikinetic aggregation, the kernel factor can be calculated from Brownian diffusion theory:

$$\beta_0 = \frac{8k_B T}{3\mu} \quad (28)$$

where  $k_B$  is the Boltzmann constant,  $T$  is the absolute temperature and  $\mu$  is the kinematic viscosity. For water at room temperature  $\beta_0$  is equal to  $10^{-17}$ . In Fig. 6 the radial-averaged mean crystal size at the reactor outlet for several  $\beta_0$ , divided by the value without aggregation, is reported. The data show that in the case of aggregation kernel equal to  $10^{-17}$  the mean crystal size increases of about 2 %. In Fig. 7 the radial-averaged total number density, divided by the value without aggregation, is reported against the aggregation kernel. These results show that also in dilute system, under these operating conditions, aggregation takes place. The local values of total number density and mean crystal size are appreciably affected by aggregation. This effect is still detectable on the radial-averaged values at the reactor outlet. Especially for the total number density the model predicts a reduction of 20 %, while for the mean crystal size the effect is lower (increase of about 1 %). Although the important simplifications that affect the model, due to the short residence time in the reactor, predictions are reasonable. An extension of the model to study the effect of aggregation during precipitation for longer residence time needs to be validated by comparison with complete solutions of population balance, using a standard technique (i.e., Monte Carlo methods).

### 3.4 Conclusion

A CFD approach coupled with a multi environment micromixing model for the sub-grid scale, was used to study the role of aggregation in precipitation process. The population balance for the solid phase was solved with the moment method and the aggregation terms were obtained under certain hypothesis. The model was applied to study the turbulent precipitation of barium sulphate in a tubular reactor with unpremixed feed. The results show that even in dilute systems, aggregation can affect the final value of total number density and mean crystal size. Although a simplified approach is employed, the results are reasonable, and show that the use of the moment method can be successfully applied to study precipitation including aggregation. The application

of the model to study aggregation for longer residence time might require a better validation and a partial reformulation of the problem. For example, the expansion of the term under the integral using the Taylor series can be done considering the coefficients as a function of CSD (i.e.,  $m_j$ ).

## Notation

$B$	birth rate due to aggregation, $1/\text{m}^3 \text{ s}$
$C_\mu$	turbulent constant
$C_\phi$	micromixing constant
$D$	death rate due to aggregation, $1/\text{m}^3 \text{ s}$
$d_{32}$	mean crystal size, m
$f_\phi(\psi; \mathbf{x}, t)$	joint probability density function
$G$	crystal growth rate, m/s
$J$	nucleation rate, $1/\text{m}^3 \text{ s}$
$k$	turbulent kinetic energy, $\text{m}^2/\text{s}^2$
$k_a$	surface shape factor
$k_d$	mass transfer coefficient, $(\text{m}/\text{s})(\text{m}^3/\text{mol})$
$k_s$	barium sulphate solubility product, $\text{mol}^2/\text{m}^6$
$k_v$	volume shape factor
$L$	particle dimension, m
$m_j$	local $j^{\text{th}}$ moment of the crystal size distribution, $\text{m}^{j-4}$
$M$	barium sulphate molecular weight, kg/mol
$n(L; \mathbf{x}, t)$	numerical crystal size distribution function, $1/\text{m}^3 \text{ m}$
$p_n$	probability of mode $n$
$s_\alpha$	weighted concentration of scalar $\alpha$ , $\text{mol}/\text{m}^3$
$s_j$	weighted $j^{\text{th}}$ moment of the crystal size distribution, $\text{m}^{j-4}$
$Sc_t$	turbulent Schmidt number
$T$	absolute temperature, k
$\langle u_i \rangle$	Reynolds averaged velocity in $i^{\text{th}}$ direction, m/s
<i>Greek Letters</i>	
$\beta$	aggregation kernel, $\text{m}^3/\text{s}$
$\phi_\alpha$	local concentration, $\text{mol}/\text{m}^3$
$\Gamma_t$	turbulent diffusivity, $\text{m}^2/\text{s}$
$\gamma_s$	micromixing rate, 1/s
$\gamma_t$	spurious dissipation rate, 1/s
$\varepsilon$	turbulent dissipation rate, $\text{m}^2/\text{s}^3$
$\mu$	dynamic viscosity, kg/ms
$\rho$	crystal density, $\text{kg}/\text{m}^3$
<i>Superscripts</i>	
$(n)$	local value in mode $n$
<i>Operators</i>	
$\langle \rangle$	Reynolds average

## References

- Baldyga, J., and W. Orciuch, "Closure Problem for Precipitation," *Trans. Inst. Chem. Eng.*, **75A**, 160 (1997).
- Baldyga, J., and W. Orciuch, "Closure Method for Precipitation in Inhomogeneous Turbulence," *Proceeding of the 14th Symposium on Industrial Crystallization*, 12-16 Sept, paper 86, Rugby, UK, 1069 (1999).
- Baldyga, J., Podgorska, W., and R. Pohorecky, "Mixing Precipitation Model with Application to Double Feed Semibatch Precipitation," *Chem. Eng. Sci.*, **50**, 1281 (1995).
- Fluent Inc. "Fluent 5 User's Guide," Fluent Inc., Lebanon, New Hampshire, USA (1990).
- Fox, R.O., "On the Relationship Between Lagrangian Micromixing Models and Computational Fluid Dynamics," *Chem. Eng. Proc.*, **37**, 521 (1998).
- Gelbard, F., and J.H. Seinfeld, "Numerical Solution of the Dynamic Equation for Particulate Systems," *J. Comp. Physics*, **28**, (1978).
- Hounslow, M.J., Ryall, R.L., and V.R. Marshall, "A Discretized Population Balance for Nucleation, Growth, and Aggregation," *AIChE J.*, **34**, 1821 (1988).
- Marchisio, D.L., R.O. Fox, and A.A. Barresi, "Simulation of Turbulent Precipitation in a Semi-Batch Taylor-Couette Reactor using Computational Fluid Dynamics," *AIChE J.*, submitted.
- Nagata, S. and, Nishikawa, paper read at the Meeting of First Pacific Chem. Eng. Congress (1975) cited from Nagata, S., *Mixing Principles and Applications*, Halsted Press (Wiley), New York (1972).
- Nielsen, A.E., "Electrolyte Crystal Growth Mechanisms," *J. Crystal Growth*, **67**, 289 (1984).
- Pagliolico, S., Marchisio, D., and A.A. Barresi, "Influence of Operating Conditions on BaSO<sub>4</sub> Crystal Size and Morphology in a Continuous Couette Precipitator," *J. Therm. Anal. Cal.*, **56**, 1423 (1999).
- Phillips, R., Rohani, S., and J. Baldyga, "Micromixing in a Single-Feed Semi-Batch Precipitation Process," *A.I.Ch.E. J.*, **45**, 82 (1999).
- Piton, D., Fox, R.O., and B. Marcant, "Simulation of Fine Particle Formation by Precipitation Using Computational Fluid Dynamics," *Canadian J. Chem. Eng.*, in press (2000).
- Randolph, A.D. and M.A. Larson, *Theory of Particulate Processes*, 2nd Ed., Academic Press, San Diego (1988).
- Rivera, T., and A.D. Randolph, "A Model for the Precipitation of Pentaerythritol Tetranitrate (PETN)," *Ind. Eng. Process Des. Dev.*, **17**, 183 (1978).
- Smoluchowski, M.Z., "Versuch einer mathematischen Theorie der Koagulationskinetik Kolloider Losunger," *Z. Phys. Chem.*, **92**, 129 (1917).